Fluorescence Study of the Three Tryptophan Residues of the Pore-Forming Domain of Colicin A Using Multifrequency Phase Fluorometry[†]

Rita Vos and Yves Engelborghs*

Laboratory for Chemical and Biological Dynamics, University of Leuven, Celestijnenlaan 200D, B-3001 Leuven, Belgium

Jacques Izard and Daniel Baty

*Centre de Biochimie et de Biologie Moléculaire, LIDSM-UPR 9027, 31 Chemin Joseph Aiguier, BP 71,
13402 Marseille, Cedex 20, France*

ABSTRACT: We have identified the steady-state and time-resolved fluorescence of the three tryptophan residues (Trp-86, Trp-130, and Trp-140) of the pore-forming domain of colicin A using site-directed mutagenesis in order to construct two- and one-tryptophan-containing mutant proteins. Fluorescence lifetimes were measured via multifrequency phase fluorometry. The fluorescence of the pore-forming domain of colicin A is dominated by Trp-140 which contributes almost 53% to the fluorescence intensity. Mutation of Trp-140 results in a decrease in fluorescence quantum yield and average lifetime. Colicin A wild-type and all mutant proteins display multiple lifetimes which belong to three different lifetime classes: 0.38–0.57 ns for τ_1, 1.6–1.87 ns for τ_2, and 3.6–4.41 ns for τ_3 at pH 5. At pH 7, the three classes are 0.64–0.89 ns for τ_1, 2.01–2.19 ns for τ_2, and 4.23–4.94 ns for τ_3. This pH effect influences all the lifetimes and must be attributed to a general conformational change. In wild-type colicin A, τ_3 originates mainly from Trp-140 while Trp-86 and Trp-130 both provide a major contribution to τ_2. The pH dependence of the fluorescence intensity gives rise to a pK_a of 5.2. The different lifetime components of two of the three single-tryptophan-containing mutants show different quenching properties toward acrylamide, indicating that each lifetime is coupled to a different microenvironment. The linear combination of the lifetimes of the single tryptophans into pairs simulates very well the behavior of the two-tryptophan-containing mutants except for one, the mutant containing Trp-86 and Trp-130. The lifetimes of the wild-type protein can only be obtained by the linear combination of the lifetimes from the mutant containing the tryptophan pair Trp-86/Trp-130 and the mutant containing Trp-140. Mutual energy transfer between Trp-86 and Trp-130 is assumed to be the explanation of this deviation since the mutant proteins display no structural or dynamic aberrances. The calculated energy transfer efficiency amounts to 65% for energy transfer from Trp-86 to Trp-130 and 21% for the reverse transfer and is in agreement with our measurements.

Fluorescence spectroscopy is a very powerful technique to monitor conformational changes in proteins. In particular, tryptophan residues are suitable intrinsic probes because of the sensitivity of the tryptophan fluorescence to the location and interactions within the protein. The assignment of the fluorescence properties (quantum yield, wavelength of fluorescence emission maximum, fluorescence lifetime) to an individual tryptophan residue is necessary for the interpretation of the observed fluorescence signals at a molecular level. The individual tryptophan fluorescence characteristics in multi-tryptophan-containing proteins can be resolved using site-directed mutagenesis to construct single-tryptophan-containing variants. However, tryptophan residues generally exhibit multiexponential fluorescence decays even in single-tryptophan-containing proteins (Beechem & Brand, 1985; Eftink, 1991). Only in a few studies of the time-resolved fluorescence of proteins and their single-tryptophan mutants is one lifetime found for one tryptophan, and the lifetimes

can be unambiguously assigned to the individual tryptophans (Waldman *et al.*, 1987; Willaert *et al.*, 1992; Shen, 1993). In most cases, the fluorescence decay of such complicated systems cannot be resolved into different constituting components. When there are no interactions between the different tryptophan residues, the fluorescence decay of a multi-tryptophan protein can be represented as a linear combination of the individual emitting tryptophans (Royer *et al.*, 1990; Axelsen *et al.*, 1991; Fetler *et al.*, 1992), and the measured decay is the weighted average of the individual decay components. This hypothesis is not valid when there are differences in structure and dynamic behavior of the mutant proteins (Royer, 1992) and/or Förster energy transfer interactions between the tryptophans (Willaert *et al.*, 1992).

In the present study, the fluorescence properties of the C-terminal domain of colicin A are determined. Colicin A is a soluble bacteriotoxin produced in the cytoplasm of *Escherichia coli* cells and then released to the extracellular medium. During the different steps of its mode of action, colicin A binds to a specific receptor located in the outer membrane of sensitive bacteria and then translocates across the membranes and finally inserts in the inner membrane to
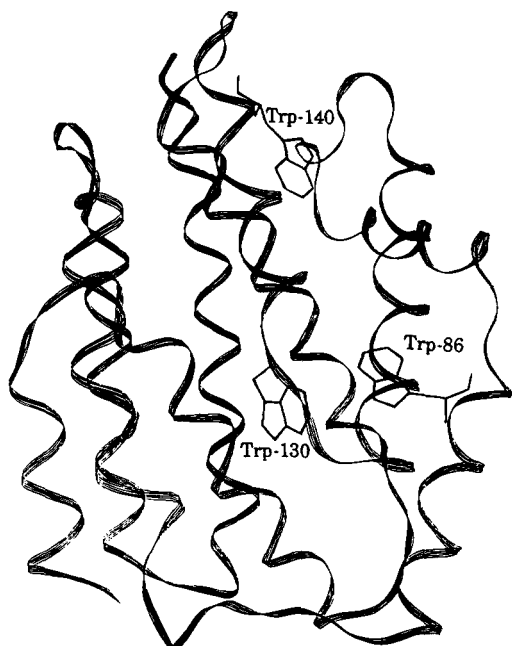
FIGURE 1: Ribbon representation of the pore-forming domain of colicin A based on the X-ray structure (Parker *et al.*, 1990, 1992) with the three tryptophan residues at positions 86, 130, and 140.

form voltage-gated ion channels (Baty *et al.*, 1990). Its 21 kDa C-terminal domain (204 amino acids) has the pore-forming activity in artificial membranes (Martinez *et al.*, 1983) and can be obtained by thermolytic digestion of colicin A purified from the extracellular medium (Tucker *et al.*, 1989). The three-dimensional structure of this soluble fragment has been obtained at 2.4 Å resolution (Parker *et al.*, 1990, 1992). The molecule consists of a bundle of 10 α-helices which are organized in three layers containing a hydrophobic helical hairpin buried within the protein.

The pore-forming domain of colicin A contains three tryptophan residues at positions 86, 130, and 140 which are localized in the hydrophobic pocket formed by helices 3−7 (see Figure 1). With the aim to determine the steady-state and time-resolved fluorescence characteristics of the different tryptophans separately, we used site-directed mutagenesis to construct two- and one-tryptophan-containing mutants by replacing selectively the tryptophans of this pore-forming domain by groups with negligible contribution to the fluorescence. The quantum yields and fluorescence emission maxima of each mutant were determined. Fluorescence lifetimes were measured via multifrequency phase fluorometry. Acrylamide quenching was used to probe the accessibility of each lifetime component to the solvent. The linear combination hypothesis—can the fluorescence decay of the whole protein be described by a simple combination of the emission of the two- and one-tryptophan-containing mutants?—was tested, and the partial failure of this hypothesis is discussed. Therefore, Förster energy transfer between the different tryptophans was calculated and compared with the experimental data.

MATERIALS AND METHODS

Bacterial Strains and Media. The *E. coli* K-12 bacterial host strain W3110 and plasmid pColA9 have been described (Lloubes *et al.*, 1986). The W3110 strain containing the various mutated plasmids was grown in LB medium. To purify the colicins, *E. coli* W3110 was grown at 37 °C to an A650 of 0.5 (5.10−8 cells/mL) in LB medium and induced 5 h with 300 ng/mL mitomycin C (MTC).

DNA Manipulation. Mutations introducing sequences recognized by restriction enzymes were obtained by site-directed mutagenesis as previously described (Baty *et al.*, 1987). Twenty oligonucleotides were used to introduce 23 unique restriction sites in the sequence coding for the C-terminal domain of colicin A (Duché *et al.*, 1994). The 38 mutated base pairs did not affect the expression nor the amino acid sequence of colicin A. All mutants were obtained by the insertion of paired oligonucleotides between restriction sites and were sequenced (manuscript in preparation). Oligonucleotides introduced TTC or TTG triplets in place of the initial triplets to code for Phe and Leu, respectively. The multiple mutants were obtained by fragment exchanges using relevant restriction sites.

Protein Purification. Five hours after induction, the culture supernatant which contained the colicin A mutant was precipitated by the addition of ammonium sulfate to 55% of saturation. The precipitate was solubilized with 10 mM phosphate buffer (pH 6.8) and dialyzed overnight against the same buffer. The colicin A wild-type and mutants were purified by a first step using an S Sepharose fast flow gel equilibrated with phosphate buffer and by a second step using a Mono S column (Pharmacia Biotech SA) equilibrated with 20 mM Mes (pH 5.5). The purified colicin was dialyzed against 20 mM Tris-HCl (pH 8.0) and treated with thermolysine as previously described (Tucker *et al.*, 1989). The hydrolysate was applied to a Superose 12 prep grade HR 16/50 column (Pharmacia Biotech SA) equilibrated with 20 mM Tris-HCl (pH 8.0). The fractions containing the colicin A thermolytic fragment were dialyzed against 50 mM ammonium bicarbonate and lyophilized before use.

Activity of Colicin A Mutants. In vivo activity of colicins was determined by measuring the changes of the K^+ concentration in the external medium with a K^+−valinomycin-selective electrode as previously described (Bourdineaud *et al.*, 1990). *E. coli* cells from the W3110 strain were grown at 37 °C to an A650 of 0.5 (5 × 10^8 cells/mL) in 2.3BT medium (5 g of bactotryptone, 8 g of nutrient broth, and 5 g of NaCl per liter, 10 mM Tris-HCl, pH 7.2, 1 mM CaCl₂). The cells were washed and resuspended in 100 mM sodium phosphate buffer (pH 7.2) and kept on ice at a density of 5 × 10^{10} cells/mL. They were used within the 2 h following their preparation as sensitive cells to measure the in vivo activity of the purified colicin. To increase the intracellular potassium concentration above 400 nmol/mg of dry weight, the cells were diluted (2 × 10^9 cells/mL) with 100 mM sodium phosphate buffer, pH 7.2, containing glucose (0.2%, w/v) and 0.5 mM KCl and incubated for 5 min at 37 °C. Colicins were added to the *E. coli* cells at a multiplicity (number of colicins per cell) of 400.

Sample Preparation. The lyophilized thermolytic fragment was dissolved in pH 5 buffer (50 mM Tris-acetate, 7.5 mM EDTA, 7.5 mM EGTA, 3 mM NaN₃). At pH 7, we used a 10 mM HEPES, 3 mM NaN₃ buffer with NaOH. The buffer solutions used at the other different pH values were a NaOAc/HOAc buffer for the region pH 4−5.5, a KH₂-PO₄/NaOH buffer for the region 6−8.5, and a Na₂B₄O₇·10H₂O/HCl buffer in the region 8−9. The ionic strength was 0.1 M with additional NaCl. All solutions were filtered before use through a 0.22 µm pore diameter filter (Millipore Co.)

to remove undissolved protein particles. The extinction coefficients of the wild-type and the different mutants were determined by the method of Gill and von Hippel (1989). For the wild-type, the extinction coefficient amounted to 23 800 M^{-1} cm^{-1}. For the double-tryptophan-containing mutants, the extinction coefficients were 12 600 M^{-1} cm^{-1} for W86F, 15 500 M^{-1} cm^{-1} for W130F, and 16 500 for W140L/K113F. For the single-tryptophan-containing mutants, the coefficients were 9450 M^{-1} cm^{-1} for W130F/W140L/K113F, 8200 M^{-1} cm^{-1} for W86F/W140L/K113F, and 7300 M^{-1} cm^{-1} for W86F/W130F at 280 nm. The concentration of the protein was never more than 40 μM to avoid aggregation.

Spectroscopic Measurements. Steady-state fluorescence spectra were obtained on a SPEX spectrofluorimeter (Fluorolog 1691). The excitation wavelength was 295 nm to minimize the contribution of tyrosyl residues to the total fluorescence. Spectra were taken with a 2 mm slit width for emission and an excitation monochromator with a wavelength resolution of 3.6 nm. The spectra were corrected for the wavelength dependence of the emission monochromator and the photomultiplier and also by substracting background intensities of the buffer solution.

The quantum yields were determined relative to tryptophan in water according to the method of Parker and Rees (1960)

$$Q_{prot} = \frac{\int I_{prot}}{\int I_{Trp}} \frac{A_{Trp}}{A_{prot}} Q_{Trp} \qquad (1)$$

where $\int I$ is the integrated intensity over the wavelength region 300−450 nm, A is the absorbance at 295 nm, and the quantum yield, Q_{Trp}, for Trp in H_2O is taken as 0.14 (Chen, 1967).

Fluorescence Lifetime Measurements. Fluorescence lifetimes were measured using multifrequency phase fluorometry (Lakowicz *et al.*, 1985). The measured phase shifts, ϕ, at a modulation frequency, ω, of the exciting light are related to the fluorescence decay in the time domain $I(t)$,

$$I(t) = \sum_i a_i \exp\left(\frac{-t}{\tau_i}\right) \qquad (2)$$

where a_i is the amplitude of the fluorescence signal of the component with lifetime τ_i, by means of the following equations (Weber, 1981):

$$\tan \phi(\omega) = \frac{S(\omega)}{G(\omega)} \qquad (3)$$

where $S(\omega)$ and $G(\omega)$ are the sine and cosine Fourier transforms of $I(t)$

$$S(\omega) = \sum_i f_i \frac{\omega \tau_i}{(1 + \omega^2 \tau_i^2)^2}$$

$$G(\omega) = \sum_i f_i \frac{1}{(1 + \omega^2 \tau_i^2)^2} \qquad (4)$$

and f_i is the steady-state contribution of the component with phase shift ϕ_i ($f_i = a_i\tau_i/\sum_i a_i\tau_i$).

An automated multifrequency phase fluorometer, as described previously by Clays *et al.* (1989), was used for the determination of fluorescence decay data. The excitation source consisted of a cavity-dumped laser (Spectra Physics 375B) with Rhodamine 6G, pumped by the 514.5 nm green line of a mode-locked Ar^+ ion laser. The dye laser pulses had a pulse width of 20 ps and a repetition frequency of 400 kHz. The excitation wavelength was 295 nm after frequency doubling, to ensure that the emission was exclusively due to tryptophan residues. The detector of the previous instrument was replaced by a fast high-gain photomultiplier (Hamamatsu H5023). A single harmonic frequency of the exciting light pulse was first converted to an intermediate frequency of 45 500 Hz via external cross-correlation, filtered, and amplified. The phase shift was measured in the low-frequency domain (700 Hz) using a second cross-correlation step. In this way, we extended the band width of our system to 1 GHz. The phase shift and its standard deviation can be accurately obtained by measuring each phase shift five times with a digital timer/counter (Philips PM 6654). NATA, with a lifetime of 2.95 ns, was used as a reference fluorophore to avoid any color effects.

Data reduction was performed on a Micro Vax 2000 minicomputer using a nonlinear least-squares algorithm (Bevington, 1969). Measurements performed at different emission wavelengths (330−370 nm) were analyzed simultaneously with global analysis in order to improve the recovery of lifetimes and amplitude fractions (Beechem *et al.*, 1983), and the data were fitted using the modified Levenberg−Marquardt algorithm (More & Sorensen, 1983) assuming fluorescence lifetimes, τ_i, which are independent of the wavelength and a variable amplitude ratio.

The solvent accessibilities of the tryptophan residues in the different mutants were probed by acrylamide-quenching experiments (Eftink & Ghiron, 1976). Measurements were performed at pH 5 and 7 by adding aliquots of a freshly prepared 8 M acrylamide stock solution to a cell containing the protein. Fluorescence lifetimes as a function of acrylamide concentration were fitted, using SigmaPlot, to

$$\frac{\tau_0}{\tau} = 1 + k_q\tau_0[Q] = 1 + K_{SV}[Q] \qquad (5)$$

where τ_0 is the lifetime in the absence of quencher and K_{SV} is the Stern−Volmer quenching constant which is equal to $k_q\tau_0$, where k_q is the bimolecular quenching rate constant.

RESULTS

Mutations and Protein Stability. Hydrophobic interactions are believed to provide a major contribution to the stabilization of proteins in an aqueous environment, and the creation of hydrophobic cavities is known to decrease the stability of proteins (Eriksson *et al.*, 1992). Moreover the predominant feature of water soluble proteins is that the nonpolar residues are buried in a core where they avoid contact with water molecules. All three tryptophan residues of the C-terminal domain of colicin A are mainly buried within the hydrophobic core of the protein. Mutation of these residues to a Phe would be destabilizing as there would be a loss of one or two hydrogen bonds and the introduction of a small hydrophobic cavity.

We assume firstly that the percentage secretion into the extracellular medium is directly related to the protein stability. Secondly, the stability is directly related to the ability of the protein to compensate for the creation of
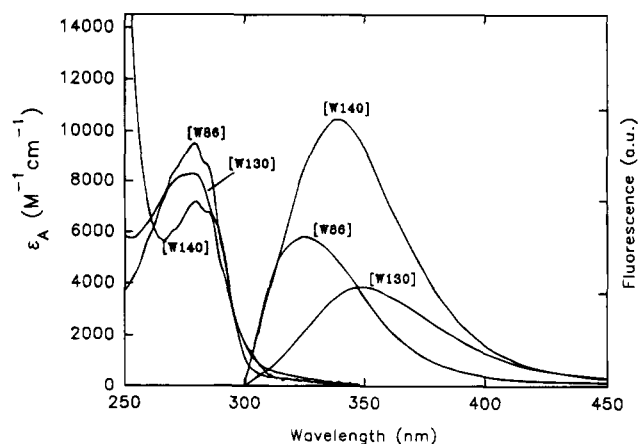
FIGURE 2: Fluorescence emission and absorption spectra of the single-tryptophan-containing mutants of the pore-forming domain of colicin A.

FIGURE 3: pH profile of the fluorescence of the pore-forming domain of colicin A (wild-type).

hydrophobic cavities by mutation. The more unstable mutants may not fold correctly and hence aggregate in the cytoplasm of the producing cell. Indeed, the W86F and W130F mutants are secreted less than the wild-type colicin A. However, the fraction secreted is large enough so that each mutant can be easily purified from the extracellular medium without using detergents and can be cleaved by thermolysin. On the other hand, the Trp-140→Phe mutation leads more drastically to aggregation probably because the Trp-140 aromatic side chain stacks against the aliphatic portion of Lys-113 and the mutation to a Phe would result in the loss of hydrogen bonds and the creation of a hydrophobic cavity. The purification of the W140F mutant from the cells needed the use of a detergent, and the protein is totally degraded by thermolysin probably because its conformation is different from the wild-type. To circumvent this problem, Trp-140 was replaced by Leu and a second mutation, Lys-113 to Phe, was introduced. The mutations of Lys-113 to Phe and Trp-140 to Leu allow the rotation of the Phe into the cavity and so partially compensate for the cavity-causing instability (unpublished result). The W140L/K113F double mutant is secreted into the extracellular medium and then purified and its C-terminal domain easily obtained by thermolytic digestion.

As can be concluded from the percentage secretion, the replacement of Trp-86 and Trp-130 by Phe does not seem to alter the structure of the protein. Contrary to the Trp-140→Phe mutation, the double mutant W140L/K113F seems to have a structure similar to the wild-type. The activity of all the mutated proteins, including W140F, determined by measure of the K⁺ efflux, is very similar to the wild-type colicin A, which suggests that the structure of the channel
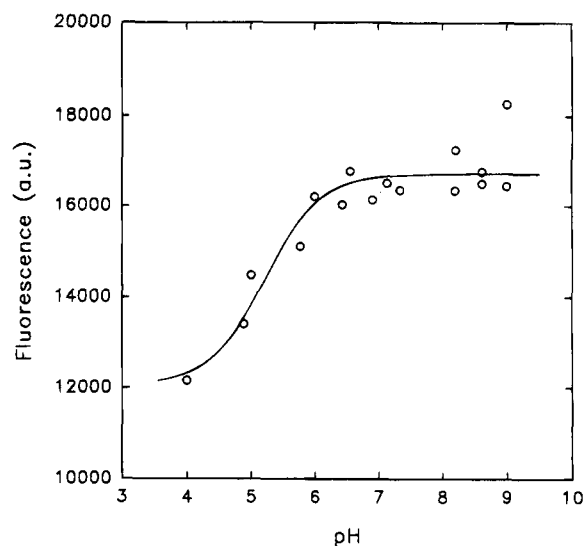
in the inner membrane of *E. coli* cells is similar to the wild-type (data not shown).

Steady-State Fluorescence Parameters. The absorption and fluorescence emission spectra of the single-tryptophan-containing mutants are shown in Figure 2. These spectra immediately show that Trp-130 is characterized by a strongly red-shifted emission (350 nm). Trp-86 shows a pronounced blue emission (325 nm), while Trp-140 has an intermediate emission maximum at 340 nm. Since the Stokes shift depends strongly on the polarity and mobility of the environment, it can be concluded that Trp-130 is in a highly polar environment, Trp-86 must be buried into the hydrophobic interior of the protein, and Trp-140 must be in an intermediate situation. Trp-140 clearly displays the highest intensity and therefore must show the highest quantum yield and highest average lifetime. This is confirmed by the data in Table 1, where the wavelength of maximum emission, the quantum yield, and the average lifetime are given for all the proteins studied. The general feature of the individual tryptophan residues are recognized in the single Trp mutants as well. Removal of Trp-86 causes a red shift of the emission maximum with respect to the wild-type. Whenever Trp-140 is removed, the quantum yield and the average lifetime drop considerably. Removal from the wild-type of Trp-86 or Trp-130 does not influence the fluorescence parameters of the wild-type substantially, indicating that its fluorescence is largely dominated by Trp-140.

The steady-state fluorescence of the pore-forming domain of colicin A wild-type as a function of pH is shown in Figure

Table 1: Wavelength of Maximum Emission, λ_{max}, Quantum Yields, Q,[a] Average Lifetime, $\langle\tau\rangle$,[b] and Radiative, k_R,[c] and Nonradiative Rate Constants, k_{NR},[d] for the Pore-Forming Domain of Wild-Type Colicin A and the Different Mutants at pH 5

protein	λ_{max} (nm)	Q	$\langle\tau\rangle$ (ns)	k_R (ns⁻¹)	k_{NR} (ns⁻¹)
WT	334	0.13 ± 0.01	3.15 ± 0.09	0.041 ± 0.005	0.28 ± 0.01
W86F	338	0.12 ± 0.01	3.05 ± 0.1	0.039 ± 0.005	0.29 ± 0.02
W130F	335	0.13 ± 0.02	3.06 ± 0.07	0.042 ± 0.008	0.28 ± 0.01
W140L/K113F	331	0.07 ± 0.01	2.3 ± 0.1	0.030 ± 0.006	0.40 ± 0.02
W86F/W130F	339	0.16 ± 0.02	3.56 ± 0.05	0.045 ± 0.006	0.24 ± 0.01
W86F/W140L/K113F	350	0.06 ± 0.02	2.07 ± 0.06	0.03 ± 0.01	0.45 ± 0.03
W130F/W140L/K113F	325	0.08 ± 0.01	2.1 ± 0.1	0.038 ± 0.007	0.44 ± 0.03

[a] Quantum yields are relative to Trp in water ($Q = 0.14$). [b] Average lifetimes are calculated from the individual lifetimes, τ_i, listed in Table 2 and the corresponding steady-state fractions, f_i, at 340 nm as $\langle\tau\rangle = \Sigma_i f_i \tau_i$. [c] $k_R = Q/\langle\tau\rangle$. [d] $k_{NR} = (1- Q)/\langle\tau\rangle$.
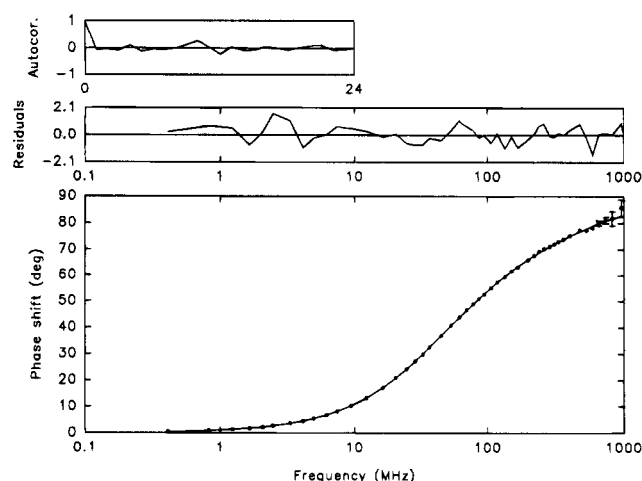
FIGURE 4: Typical phase measurement of wild-type C-terminal domain of colicin A at pH 5 and graphical tests incorporated in the data analysis. Measured phase angles (●) are plotted as a function of frequency and fitted for a sum of three exponentials. Also included are plots of the weighted residuals versus frequency and of their autocorrelation function.

3. The fluorescence intensity is found to be dependent upon pH with an apparent pK_a of 5.2.

Fluorescence Lifetimes. The fluorescence decay parameters were determined at emission wavelengths ranging from 330 to 370 nm in 5 nm intervals. Best fit (lowest χ_R—no systematic deviation in the autocorrelation function or the weighted residuals) was obtained with a triple-exponential fit (Figure 4). In order to increase the accuracy of the recovery of the lifetimes and the fractional intensities, a global analysis of all the phase measurements at the different wavelengths was performed. This means that all the phase data were fitted with a single set of three lifetimes and at each wavelength a separate set of three amplitude fractions. The result of this global analysis is shown in Table 2. For the mutant W86F/W130F, the fluorescence decay can only be described by two exponentials. Possibly, τ_2 contains an unresolved fraction of a short component.

Decay-associated spectra of the different lifetimes can be obtained by multiplying the fractional contribution of each lifetime with the steady-state emission intensity at each wavelength. These spectra, which display the heterogeneity of the fluorescence emission, are given in Figure 5. In wild-type C-terminal fragment colicin, τ_3 originates mainly from Trp-140, while Trp-86 and Trp-130 both provide a major

contribution to τ_1 and τ_2. When applied to single-tryptophan proteins (the lowest row of Figure 5), these data reveal that the spectra associated with the different lifetimes of a single tryptophan are associated with different Stokes shifts. The shortest lifetimes always contribute the most at shorter wavelengths, whereas the long-lived components are red-shifted. The intermediate lifetime τ_2 of Trp-130 in the mutant W86F/W140L/K113F is shifted to the red. When Trp-130 is mutated (W130F; W86F/W130F; W130F/W140L/K113F), this shift is absent.

Acrylamide Quenching of the Lifetimes. The susceptibility of the fluorescence lifetimes to quenching by acrylamide was used to probe the solvent accessibility of the tryptophan residues. These quenching experiments allow the determination of the rate constant for collisions between the quencher and the fluorescent group. For a fully exposed tryptophan residue (*e.g.*, free Trp in water), this value can be as high as $6.4 \text{ M}^{-1} \text{ ns}^{-1}$. A value smaller than this upper limit is interpreted as an indication for a lower accessibility of the tryptophan. Fluorescence-quenching experiments with acrylamide were performed at pH 5 and 7. Figure 6 shows the Stern—Volmer plots for acrylamide quenching of the lifetimes of the pore-forming domain of colicin A wild-type. At pH 5, the values for the bimolecular quenching constant, k_q, are $0.46 \pm 0.18 \text{ ns}^{-1} \text{ M}^{-1}$ for τ_1, $0.213 \pm 0.003 \text{ ns}^{-1} \text{ M}^{-1}$ for τ_2, $0.259 \pm 0.004 \text{ ns}^{-1} \text{ M}^{-1}$ for τ_3, and $0.30 \pm 0.01 \text{ ns}^{-1} \text{ M}^{-1}$ for the mean lifetime, $\langle \tau \rangle$. K_{SV} amounts to $0.99 \pm 0.03 \text{ M}^{-1}$ for $\langle \tau \rangle$, which is in agreement with the value of 1.07 obtained by Lakey *et al.* (1991) from fluorescence intensity-quenching experiments. At pH 7, the values are $0.42 \pm 0.06 \text{ ns}^{-1} \text{ M}^{-1}$ for τ_1, $0.201 \pm 0.005 \text{ ns}^{-1} \text{ M}^{-1}$ for τ_2, $0.23 \pm 0.01 \text{ ns}^{-1} \text{ M}^{-1}$ for τ_3, and $0.28 \pm 0.01 \text{ ns}^{-1} \text{ M}^{-1}$ for the mean lifetime, $\langle \tau \rangle$, indicating that there is a slight decrease in the solvent accessibility at pH 7 for all the lifetimes in the wild-type.

The bimolecular quenching constants, k_q, corresponding to τ_2 and τ_3 for the different mutant proteins are shown in Table 3. The shortest lifetime τ_1, however, cannot be accurately determined at higher acrylamide concentrations, resulting in too large errors on the k_q values. Trp-130 and Trp-140 show large differences in k_q for the two lifetimes in contrast to Trp-86.

DISCUSSION

Environment of the Three Tryptophan Residues in the C-Terminal Domain of Colicin A. Examination of the three-

Table 2: Results of the Global Analysis of the Fluorescence Decay of the C-Terminal Domain of Colicin A and Two- and One-Tryptophan-Containing Mutants[a]

|	τ_1 (ns)	τ_2 (ns)	τ_3 (ns)	a_1	a_2	a_3	χ_R^2
			pH 5				
WT	0.57 ± 0.02	1.77 ± 0.04	3.95 ± 0.02	0.21 ± 0.01	0.40 ± 0.01	0.39 ± 0.01	1.1
W86F	0.38 ± 0.02	1.78 ± 0.05	3.95 ± 0.04	0.30 ± 0.01	0.38 ± 0.01	0.32 ± 0.01	0.9
W130F	0.55 ± 0.02	1.87 ± 0.04	3.99 ± 0.09	0.20 ± 0.03	0.45 ± 0.01	0.35 ± 0.01	1.1
W140L/K113F	0.49 ± 0.02	1.68 ± 0.04	3.82 ± 0.08	0.31 ± 0.02	0.54 ± 0.02	0.15 ± 0.01	1.7
W86F/W130F	–	1.60 ± 0.02	4.06 ± 0.01	–	0.41 ± 0.01	0.59 ± 0.01	1.5
W86F/W140L/K113F	0.43 ± 0.01	1.73 ± 0.03	3.58 ± 0.12	0.38 ± 0.01	0.53 ± 0.01	0.09 ± 0.01	1.4
W130F/W140L/K113F	0.44 ± 0.01	1.78 ± 0.01	4.41 ± 0.07	0.17 ± 0.01	0.78 ± 0.01	0.05 ± 0.01	3.6
			pH 7				
WT	0.75 ± 0.03	2.19 ± 0.08	4.37 ± 0.06	0.24 ± 0.02	0.44 ± 0.01	0.32 ± 0.01	0.9
W130F	0.64 ± 0.03	2.12 ± 0.09	4.23 ± 0.06	0.22 ± 0.01	0.42 ± 0.01	0.36 ± 0.01	2
W140L/K113F	0.72 ± 0.02	2.01 ± 0.04	4.89 ± 0.09	0.33 ± 0.01	0.57 ± 0.01	0.1 ± 0.01	3
W130F/W140L/K113F	0.89 ± 0.07	2.08 ± 0.06	4.94 ± 0.31	0.19 ± 0.03	0.76 ± 0.02	0.05 ± 0.01	1.6

[a] Amplitude fractions at 340 nm.
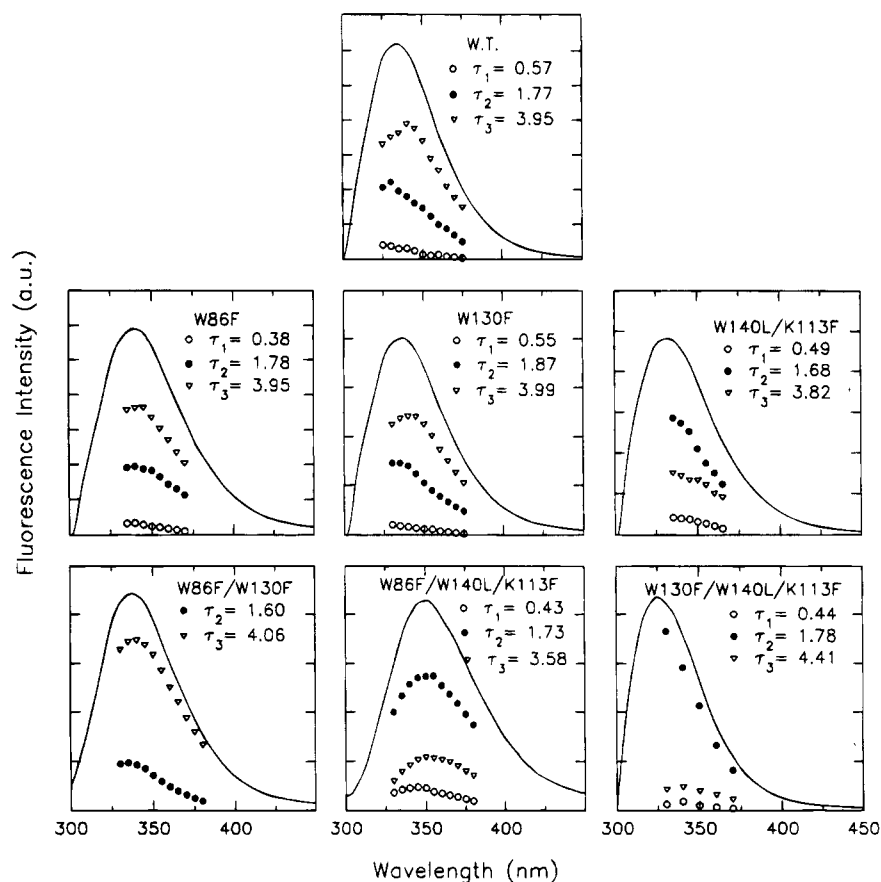
FIGURE 5: Decay-associated spectra of the wild-type and the different mutants of the pore-forming domain of colicin A at pH 5.
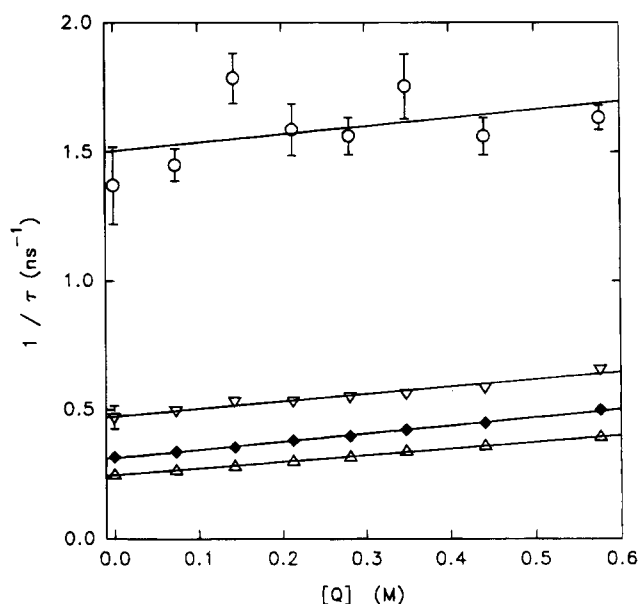

FIGURE 6: Stern—Volmer quenching plots of the pore-forming domain of colicin A wild-type at pH 5. Key to plot: τ_1 (O), τ_2 (∇), τ_3 ($\triangle$), and $\langle\tau\rangle$ ($\blacklozenge$).

dimensional structure of the C-terminal domain of colicin A (Figure 1) reveals that all three tryptophan residues are almost completely buried in the hydrophobic interior of the protein. The solvent accessible areas of the indole rings of the three tryptophans were calculated using an analytical algorithm (Alard, 1991) implemented in Brugel (UsrConsult, Belgium) and amount to 0.025 Å^2 for Trp-86, 6.9 Å^2 for Trp-130, and 8.5 Å^2 for Trp-140. For reference, the total accessible area of a tryptophan side chain amounts to 266

Å^2 (probe radius, 1.6 Å). Qualitatively, the calculated values are in agreement with the experimental solvent accessibilities as probed by acrylamide quenching, namely, the most buried, Trp-86, displays the smallest bimolecular quenching constant while the more accessible residues, Trp-130 and Trp-140, show larger quenching constants.

The amino acids in the proximity of the tryptophan side chains are known from the crystal structure and are represented in Figure 7 using the software program WhatIf (Vriend, 1990). Both Trp-86 and Trp-130 are for the most part surrounded by hydrophobic apolar amino acids, with no charged amino acids in the immediate environment. The side chain of Trp-86 stacks parallel against Tyr-161 and is within hydrogen bond distance of the side chain hydroxyl groups of Tyr-161 and Ser-121. Trp-130 is located perpendicular to the aromatic ring of Tyr-125. In the neighborhood of Trp-140, however, there is a negative charge of the carboxylate group of Glu-136 which is pointing perpendicular toward the pyrrole part of the indole side chain of Trp-140 (distance between Nϵ atom of Trp-140 and carboxylate of Glu-136 amounts of 3.1 Å), while the positive charge of Lys-113 is pointing toward the Cβ atom of the tryptophan residue at a distance of 4.5 Å.

The fluorescence emission spectrum is generally an indication of the polarity of the environment of the tryptophan residues. The contribution of water to the polarity of the environment is given by the acrylamide-quenching constants and the solvent accessible areas as described above. Trp-86, which is totally buried, displays the biggest blue shift in the emission spectrum. Trp-130 and Trp-140 are more accessible for the solvent, and their fluorescence spectrum is consequently red-shifted. Also charges located on side

Table 3: Bimolecular Quenching Rate Constants, k_q, as Obtained from the Acrylamide Quenching at pH 5

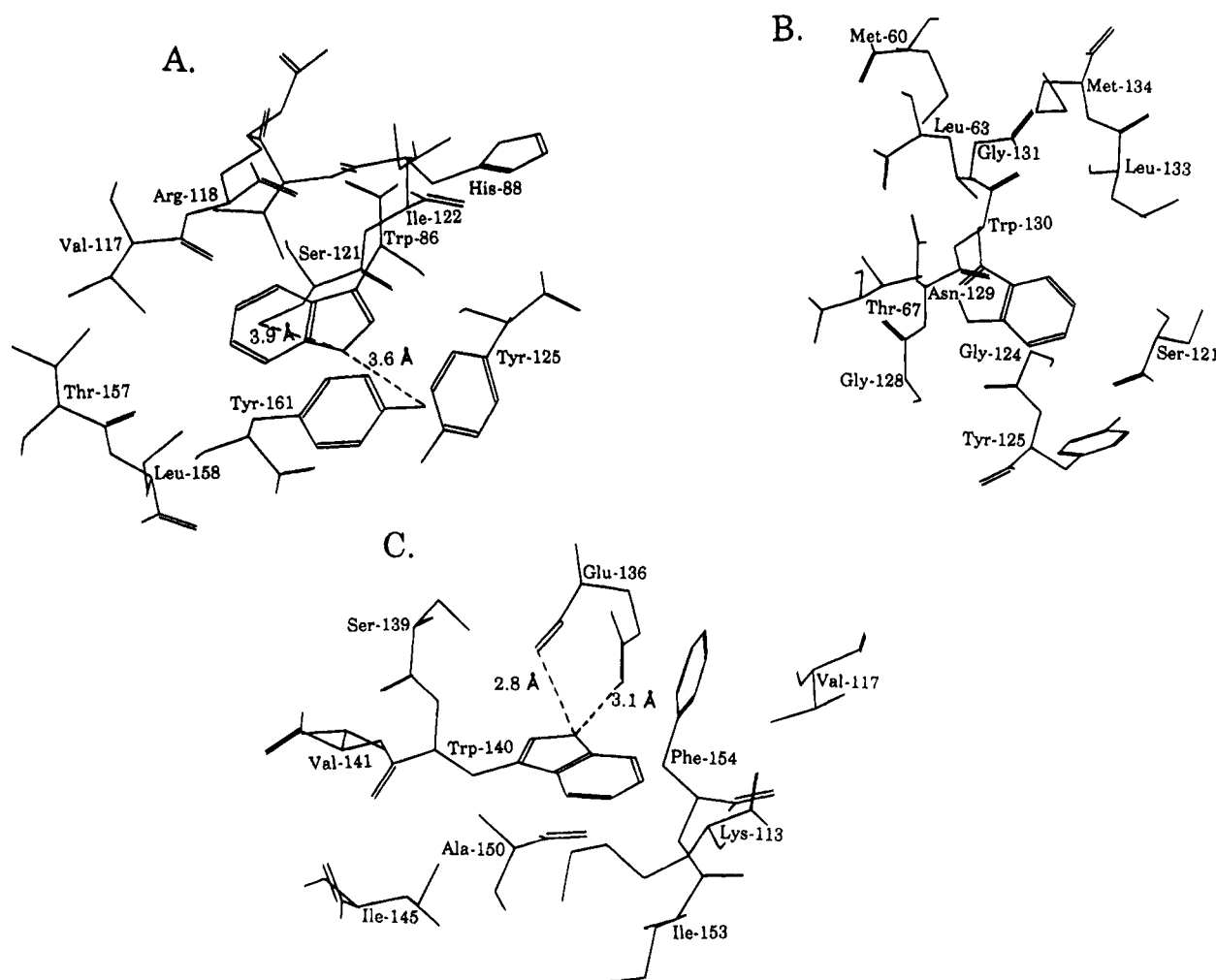|	k_q (ns^{-1} M^{-1})		
	τ_2	τ_3	$\langle \tau \rangle$
WT	0.21 ± 0.01	0.26 ± 0.01	0.30 ± 0.01
W86F	1.4 ± 0.4	0.30 ± 0.02	0.36 ± 0.02
W130F	0.21 ± 0.06	0.22 ± 0.02	0.27 ± 0.01
W140L/K113F	0.63 ± 0.09	0.19 ± 0.03	0.29 ± 0.01
W86F/W130F	1.1 ± 0.5	0.28 ± 0.02	0.32 ± 0.01
W86F/W140L/K113F	1.19 ± 0.09	0.07 ± 0.02	0.38 ± 0.02
W130F/W140L/K113F	0.2 ± 0.07	0.19 ± 0.01	0.23 ± 0.01

FIGURE 7: Close-up view of the amino acids in the environment of the three tryptophan residues: (A) Trp-86, (B) Trp-130, and (C) Trp-140.

chains of amino acids in the proximity of the indole moiety influence the polarity and can provoke a shift in the spectrum. In order to assess the exact effect of their presence, more extensive calculations are required (Ilich *et al.*, 1988). However, in the first instance, it seems that the wavelength of maximum fluorescence emission is proportional with the solvent accessibility.

The radiative rate constants, k_R ($k_R = 1/\tau_R = Q/\langle \tau \rangle$), and nonradiative rate constants, k_{NR} ($k_{NR} = (1 - Q)/\langle \tau \rangle$), are given in Table 1. The radiative rate constant, k_R, of indole is dependent upon the polarity of the environment and is higher in nonpolar solvents than in water (Privat *et al.*, 1979). Also the direction of the electric field in the vicinity of the tryptophan side chain is important (Ilich *et al.*, 1988; Szabo & Faerman, 1992). For the residues Trp-86 and Trp-130,

we find $k_{R,Trp-86} > k_{R,Trp-130}$ in accordance with the polarity defined as $\lambda_{max,Trp-86} < \lambda_{max,Trp-130}$.

The radiative rate constant of Trp-140 is unexpectedly high. This may be due to the presence of the charges in the vicinity of the indole side chain of Trp-140 which can influence the radiative rate constant via the oscillator strength of the transition (Ilich *et al.*, 1988). The increase in the mean fluorescence lifetime, $\langle \tau \rangle$, for Trp-140 originates from a marked decrease in the nonradiative rate constant, k_{NR}. We assume that this may be due to the presence of the carboxylate group of Glu-136. Indeed, the tryptophan derivative indole-3-propionic acid, which contains only a CO_2^- on the α-carbon, displays a long fluorescence lifetime with a low nonradiative rate constant comparable to the value of k_{NR} for 3-methylindole (Szabo & Rayner, 1980).

Table 4: Lifetimes and Amplitudes Calculated from the Sum of the Decays of the Individual Tryptophans or Tryptophan Pairs

protein		τ_1 (ns)	τ_2 (ns)	τ_3 (ns)	a_1	a_2	a_3	$\langle\tau\rangle$ (ns)
W86F	exptl	0.38	1.78	3.95	0.30	0.38	0.32	3.05
	a	0.43	1.67	4.02	0.16	0.46	0.38	3.15
W130F	exptl	0.55	1.87	3.99	0.20	0.45	0.35	3.06
	b	0.44	1.73	4.09	0.09	0.60	0.31	2.98
W140L/K113F	exptl	0.49	1.68	3.82	0.31	0.54	0.15	2.32
	c	0.43	1.76	4.00	0.25	0.68	0.07	2.07
WT	exptl	0.57	1.77	3.95	0.21	0.40	0.39	3.16
	d	0.43	1.73	4.05	0.16	0.59	0.25	2.81
	e	0.49	1.81	3.94	0.27	0.48	0.25	2.78
	f	0.49	1.66	3.99	0.19	0.44	0.37	3.11
	g	0.39	1.78	3.89	0.25	0.54	0.21	2.63

[a] Calculated as W86F/W140L/K113F + W86F/W130F. [b] W130F/W140L/K113F + W86F/W130F. [c] W130F/W140L/K113F + W86F/W140L/K113F. [d] W130F/W140L/K113F + W86F/W140L/K113F + W86F/W130F. [e] W86F/W140L/K113F + W130F. [f] W86F/W130F + W140L/K113F. [g] W130F/W140L/K113F + W86F.

Heterogeneous Decay in the Pore-Forming Domain of Colicin A and Its One- and Two-Tryptophan-Containing Mutants. The C-terminal domains of colicin A wild-type and all mutant forms display multiexponential decay kinetics with lifetimes belonging to three different lifetime classes: 0.38–0.57 ns for τ_1, 1.6–1.87 ns for τ_2, and 3.6–4.41 ns for τ_3 at pH 5. At pH 7, the three classes are 0.64–0.89 ns for τ_1, 2.01–2.19 ns for τ_2, and 4.23–4.94 ns for τ_3.

This decrease in all lifetimes at pH 5 compared to pH 7 must be provoked by a general effect, *e.g.*, an increase in quenching by the solvent or protein matrix. At acidic pH, it is known that the pore-forming domain is destabilized, resulting in a looser and more flexibe 'molten globule' intermediate (van der Goot *et al.*, 1991; Muga *et al.*, 1993) which facilitates the membrane insertion (Pattus *et al.*, 1983). However, no conformational changes, or a change in the secondary structure associated with this increased affinity at pH 5, were detected previously by other spectroscopic techniques (Lakey *et al.*, 1991; Goormaghtigh *et al.*, 1991). We found that at pH 5 the three tryptophans are slightly more accessible to the quencher compared to at pH 7, indicating that the tryptophan residues located in the hydrophobic core of colicin A are more exposed to the solvent, which results in a decrease in all lifetimes.

An alternative explanation for this phenomenon could be that in the neighborhood of Trp-86 there is a histidine residue (His-88), which can provoke the decrease in lifetime upon acidification. However, the pH dependence of the fluorescence of the C-terminal domain of colicin A reveals an apparent pK_a of 5.2 which is unusually low for a histidine residue. Moreover, His-88 points away from the tryptophan residues and can not collide, which is essential for an efficient quenching (Vos & Engelborghs, 1994).

Complex fluorescence decays in proteins are usually explained by different conformations, resulting in different interactions of the tryptophan side chain with amino acid groups of the surrounding protein matrix [see, *e.g.*, Petrich *et al.* (1983), Hutnik and Szabo (1989), Kim *et al.* (1993)]. The longer lifetimes are thought to originate from conformations with little interaction with the environment, while the shorter lifetimes are the result of dynamic quenching from the solvent or the protein matrix. Recently, Bajzer and Prendergast (1993) developed an alternative model to describe the multiexponential fluorescence decay of tryptophan in proteins because in many proteins there seems to be no basis for assuming multiple tryptophan conformations

since they would disrupt the closely packed protein matrix. Their model is based on the occurrence of transfer of the excited-state energy from the fluorophore to acceptors located elsewhere in the protein matrix. So far we have not found indications for these energy acceptors.

We therefore assume that multiple protein microconformations are on the origin of multiexponential fluorescence decay in proteins. Each lifetime corresponds to a distinguishable conformational state which can be characterized by a bimolecular quenching constant and an associated spectrum. The quenching constant, k_q, for the single-tryptophan-containing mutant forms increases in the order $\tau_3 < \tau_2$. The long-lived component τ_3 originates from a 'relaxed' conformation (spectrum is shifted to lower energy) with low accessibilities for the solvent. Consequently, the red shift of this component must be caused by relaxation of the protein matrix around the excited state. In many proteins, it is known that dipolar relaxation of the protein matrix is on the order of nanoseconds (Demchenko *et al.*, 1993). Trp-86, which is located in a more rigid and more nonpolar environment and hence thought to be not susceptible to these relaxation processes, displays negligible shifts in the amplitudes as a function of wavelength. The relative amplitudes corresponding to the lifetimes of the more polar residues Trp-130 and Trp-140 exhibit a more pronounced shift in their spectra.

Could the Wild-Type Fluorscence Be Represented by the Sum of the Emissions of the Individual Tryptophans? The lifetimes, τ_i (i = 1, 2, and 3), of the wild-type and the two-tryptophan-containing mutants were calculated from the lifetimes, τ_i, and amplitude fractions, a_i, of the separate tryptophans or tryptophan pairs according to

$$\langle\tau_i\rangle = \sum_j \frac{a_j\epsilon_j}{\tau_{R,j}}\tau_j^2 \Big/ \sum_j \frac{a_j\epsilon_j}{\tau_{R,j}}\tau_j \tag{6}$$

with j being each individual mutant. The pre-exponential factors of the fluorescence decay of each tryptophan need to be weighted by ϵ/τ_R, with ϵ being the absorbance of the respective tryptophan and τ_R its radiative lifetime which is calculated from the quantum yield, ϕ, and the mean lifetime, $\langle\tau\rangle$, as $\langle\tau\rangle/\phi$. The result is given in Table 4. Best fit is obtained for W130F, W86F, and wild-type calculated from the fluorescence decay of respectively Trp-86 + Trp-140, Trp-130 + Trp-140, Trp-140, and the tryptophan pair Trp-86/Trp-130. The fluorescence of the tryptophan pair Trp-

Table 5: Calculated Distances, R (Å), Orientation Factors, κ^2, Overlap Integrals, J_{AD} (10^{-16} cm^6 mmol^{-1}), R_0 Values (Å), and Energy Transfer Efficiencies, E (%), for the Different Tryptophan Pairs in the Pore-Forming Domain of Colicin A

	86→130	130→86	130→140	140→130	86→140	140→86
R	10.09	10.09	15.82	15.82	14.18	14.18
κ^2	0.59	0.59	6.13×10^{-3}	6.13×10^{-3}	4.09×10^{-5}	4.09×10^{-5}
J_{AD}	2.44	0.46	0.71	0.83	1.82	1.54
R_0	11.23	8.11	4.07	4.97	2.16	2.39
E	0.65	0.21	2.89×10^{-4}	9.57×10^{-4}	1.3×10^{-5}	2.29×10^{-5}

Table 6: Calculated Lifetimes ($1/\lambda_+$ and $1/\lambda_-$) from the Combination of the Lifetimes of the Mutants W130F/W140L/K113F (Trp-86) and W86F/W140L/K113F (Trp-130) with Energy Transfer Rate Constants of 1.86 and 0.36 ns^{-1} for, Respectively, $k_{86\to130}$ and $k_{130\to86}$, According to Formula 12 (Porter, 1972)

		lifetimes of Trp-86 ($1/k_{86}$)		
		$\tau_1 = 0.44$ ns	$\tau_2 = 1.78$ ns	$\tau_3 = 4.41$ ns
lifetimes of Trp-130 ($1/k_{130}$)	$\tau_1 = 0.43$ ns	0.13 and 0.43	0.27 and 0.86	0.30 and 1.94
	$\tau_2 = 1.73$ ns	0.15 and 1.51	0.52 and 1.74	0.87 and 2.58
	$\tau_3 = 3.58$ ns	0.15 and 3.92	0.59 and 3.34	1.31 and 3.72

86/Trp-130 can not be represented by the sum of the decays of the individual tryptophans. This is most obvious in the average lifetime, $\langle\tau\rangle$, in the longest lifetime, τ_3, and in the corresponding amplitude fraction, a_3. Since there are no structural or dynamic aberrances, we interpret this as an indication for energy transfer between Trp-86 and Trp-130.

According to Förster's classic theory (Förster, 1948), the energy transfer between the three tryptophan residues can be calculated from the known crystal structure. The efficiency of radiationless energy transfer, E, between a donor, D, and an acceptor, A, is given by

$$E = \frac{R_0^6}{R_0^6 + R^6} \qquad (7)$$

where R is the distance between the donor and the acceptor.

The distance, R_0 (in cm), at which 50% energy transfer occurs is obtained from

$$R_0^6 = (8.79 \times 10^{-25})(n^{-4}\phi_D\kappa^2 J_{AD}) \qquad (8)$$

The refractive index, n, of the medium is taken as 1.5 (Desie et al., 1986). ϕ_D is the quantum yield of the donor in the absence of the acceptor and is taken from Table 1.

The geometric dipole−dipole orientation factor, κ^2, is calculated from

$$\kappa^2 = (\cos\theta_T - 3\cos\theta_D\cos\theta_A)^2 \qquad (9)$$

where θ_T is the angle between the emission dipole of the donor and the absorption dipole of the acceptor and θ_D and θ_A are the angles between these dipoles and the vector joining the midpoints of the CE2/CD2 bond of the donor and the acceptor, respectively. The direction of the transition moment of the ^1L_a state is situated $-38°$ from the longest axis in tryptophan (Yamamoto & Tanaka, 1972). The ^1L_b state is ignored in the calculation of the geometric orientation factor since absorption and fluorescence at 295 nm are mainly due to the ^1L_a state transitions [see, e.g., Harris and Hudson (1990)].

J_{AD} is the spectral overlap integral (in M^{-1} cm^3) between the emission spectrum of the donor [$F_D(\lambda)$] and the absorption spectrum of the acceptor [$\epsilon_A(\lambda)$] and is defined as

$$J_{AB} = \frac{\int F_D(\lambda)\epsilon_A(\lambda)\lambda^4 \, d\lambda}{\int F_D(\lambda) \, d\lambda} \qquad (10)$$

Values for the calculated distances R between the tryptophan residues, the orientation factors κ^2, the overlap integrals J_{AD}, and the amount of energy transfer between the three tryptophan residues are shown in Table 5. These calculations show that only between Trp-86 and Trp-130 is there an appreciable extent of energy transfer; this in accordance with what we noticed before. Between Trp-140 and the other residues, there is no significant energy transfer due to an unfavorable orientation of the tryptophan side chains (low κ^2).

The energy transfer efficiencies between Trp-86 and Trp-130 can also be written as

$$E_{86\to130} = \frac{k_{86\to130}}{k_{86} + k_{86\to130}}$$

$$E_{130\to86} = \frac{k_{130\to86}}{k_{130} + k_{130\to86}} \qquad (11)$$

where k_{86} and k_{130} are the inverse lifetimes in the absence of energy transfer and $k_{86\to130}$ and $k_{130\to86}$ are the rate constants for the forward and backward energy transfer between the residues Trp-86 and Trp-130. Taking for k_{86} and k_{130} the inverse average lifetimes, the rate constants $k_{86\to130}$ and $k_{130\to86}$ can be calculated and amount to 1.86 and 0.36 ns^{-1}, respectively. According to the formulae of Porter (1972), these rate constants will combine with the fluorescence decay constants yielding two new lifetimes ($1/\lambda_+$ and $1/\lambda_-$) which will be observable in the presence of this forward and backward energy transfer:

$$2\lambda_\pm = (k_{86} + k_{130} + k_{86\to130} + k_{130\to86}) \pm [(k_{86} + k_{130} + k_{86\to130} + k_{130\to86})^2 + 4k_{86\to130}k_{130\to86}]^{1/2} \qquad (12)$$

The result of the combination of the lifetimes of the single-tryptophan-containing mutants W130F/W140L/K113F and W86F/W140L/K113F with $k_{86\to130}$ and $k_{130\to86}$ is given in Table 6. All possible combinations are presented. By comparing with the lifetimes of the Trp-86/Trp-130 pair in W140L/K113F, it becomes clear that the combinations that

best fit the observed lifetimes for the mutant are $\tau_2 \leftrightarrow \tau_2$ and $\tau_3 \leftrightarrow \tau_3$. This shows that the lifetimes in the mutant W140L/K113F can originate very likely from such a two-way energy transfer.

ACKNOWLEDGMENT

REFERENCES

Alard, P. (1991) Ph.D. Thesis, Université Libre de Bruxelles.

Axelsen, P. H., Bajzer, Z., Prendergast, F. G., Cottam, P. F., & Ho, C. (1991) *Biophys. J. 60*, 650−659.

Bajzer, Z., & Prendergast, F. G. (1993) *Biophys. J. 65*, 2313−2323.

Baty, D., Knibiehler, M., Verheij, H., Pattus, F., Shire, D., Bernadac, A., & Lazdunski, C. (1987) *Proc. Natl. Acad. Sci. U.S.A. 84*, 1152−1156.

Baty, D., Pattus, F., Parker, M., Benedetti, H., Frenette, M., Bourdineaud, J.-P., Cavard, D., Knibiehler, M., & Lazdunski, C. (1990) *Biochimie 72*, 123−130.

Beechem, J. M., & Brand, L. (1985) *Annu. Rev. Biochem. 54*, 43−71.

Beechem, J. M., Knutson, J. R., Ross, J. B. A., Turner, B. W., & Brand, L. (1983) *Biochemistry 22*, 6054−6058.

Bevington, P. R. (1969) *Data reduction and error analysis for physical sciences*, McGraw-Hill, New York.

Bourdineaud, J.-P., Boulanger, P., Lazdunski, C., & Letellier, L. (1990) *Proc. Natl. Acad. Sci. U.S.A. 87*, 1037−1041.

Chen, R. F. (1967) *Anal. Lett. 1*, 35−42.

Clays, K., Jannes, J., Engelborghs, Y., & Persoons, A. (1989) *J. Phys. E: Sci. Instrum. 22*, 297−305.

Demchenko, A. P., Apell, H.-J., Stürmer, W., & Feddersen, B. (1993) *Biophys. Chem. 48*, 135−147.

Desie, G., Boens, N., & De Schryver, F. C. (1986) *Biochemistry 25*, 8301−8308.

Duché, D., Parker, M. W., Gonzales-Manas, J.-M., Pattus, F., & Baty, D. (1994) *J. Biol. Chem. 269*, 6332−6339.

Eftink, M. R. (1991) Fluorescence techniques for studying protein structure. in *Protein Structure Determination: Methods of Biochemical Analysis* (Suelter, C. H., Ed.) Vol. 35, pp 127−205, John Wiley & Sons, Inc., New York.

Eftink, M. R., & Ghiron, C. A. (1976) *Biochemistry 15*, 672−680.

Eriksson, A. E., Baase, W. A., Zhang, X.-J., Heinz, D. W., Blaber, M., Baldwin, E. P., & Matthews, B. W. (1992) *Science 255*, 178−183.

Fetler, L., Tauc, P., Hervé, G., Ladjimi, M. M., & Brochon, J. C. (1992) *Biochemistry 31*, 12504−12513.

Förster, T. (1948) *Ann. Phys. (Leipzig) 2*, 55−75.

Gill, S. C., & Von Hippel, P. H. (1989) *Anal. Biochem. 182*, 319−326.

Goormaghtigh, E., Vigneron, L., Knibiehler, M., Lazdunski, C., &

Ruysschaert, J. M. (1991) *Eur. J. Biochem. 202*, 1299−1305.

Harris, D. L., & Hudson, B. S. (1990) *Biochemistry 29*, 5276−5285.

Hutnik, C. M., & Szabo, A. G. (1989) *Biochemistry 28*, 3923−3934.

Ilich, P., Axelsen, P., & Prendergast, F. G. (1988) *Biophys. Chem. 29*, 341−349.

Kim, S. J., Chowdhury, F. N., Stryewski, W., Younathan, E. S., Russo, P. S., & Barkley, M. D. (1993) *Biophys. J. 65*, 215−226.

Lakey, J. H., Massotte, D., Heitz, F., Dasseux, J. L., Faucon, J. F., Parker, M. W., & Pattus, F. (1991) *Eur. J. Biochem. 196*, 599−607.

Lakowicz, J. R., Maliwal, B. P., & Gratton, E. (1985) *Anal. Instrum. 14*, 193−223.

Lloubes, R., Baty, D., & Lazdunski, C. (1986) *Nucleic Acids Res. 14*, 2621−2636.

Martinez, C., Lazdunski, C., & Pattus, F. (1983) *EMBO J. 2*, 1501−1507.

More, J. J., & Sorensen, D. C. (1983) *SIAM J. Sci. Stat. Comput. 4*, 553−572.

Muga, A., Gonzales-Manas, J. M., Lakey, J. H., Pattus, F., & Surewicz, W. K. (1993) *J. Biol. Chem. 268*, 1553−1557.

Parker, C. A., & Rees, W. T. (1960) *Analyst 85*, 587−600.

Parker, M. W., Tucker, A. D., Tsernoglou, D., & Pattus, F. (1990) *Trends Biochem. Sci. 15*, 126−129.

Parker, M. W., Postma, J. P. M., Pattus, F., Tucker, A. D., & Tsernoglou, D. (1992) *J. Mol. Biol. 224*, 639−657.

Pattus, F., Martinez, M. C., Dargent, B., Cavard, D., Verger, R., & Lazdunski, C. (1983) *Biochemistry 22*, 5698−5707.

Petrich, J. W., Chang, M. C., McDonald, D. B., & Fleming, G. R. (1983) *J. Am. Chem. Soc. 105*, 3824−3836.

Porter, G. B. (1972) *Theor. Chim. Acta 24*, 265−270.

Privat, J.-P., Wahl, P., & Auchet, J.-C. (1979) *Biophys. Chem. 9*, 223−233.

Royer, C. A. (1992) *Biophys. J. 63*, 741−750.

Royer, C. A., Gardner, J. A., Beechem, J. M., Brochon, J. C., & Mathews, K. S. (1990) *Biophys. J. 58*, 363−378.

Shen, W. H. (1993) *Biochemistry 32*, 13925−13932.

Szabo, A. G., & Rayner, D. M. (1980) *J. Am. Chem. Soc. 102*, 554−563.

Szabo, A. G., & Faerman, C. (1992) in *Time-Resolved Laser Spectroscopy in Biochemistry III* (Lakowicz, J. R., Ed.) pp 70−80, SPIE, Bellingham, WA.

Tucker, A. D., Baty, D., Parker, M. W., Pattus, F., Lazdunski, C., & Tsernoglou, D. (1989) *Protein Eng. 2*, 399−405.

Van der Goot, F. G., Gonzales-Manas, J. M., Lakey, J. H., & Pattus, F. (1991) *Nature 354*, 408−410.

Vriend, G. (1990) *J. Mol. Graph. 8*, 52−56.

Vos, R., & Engelborghs, Y. (1994) *Photochem. Photobiol. 60*, 24−32.

Waldman, A. D. B., Clarke, A. R., Wigley, D. B., Hart, K. W., Chia, W. N., Barstow, D., Atkinson, T., Munro, I., & Holbrook, J. (1987) *Biochim. Biophys. Acta 913*, 66−71.

Weber, G. (1981) *J. Phys. Chem. 85*, 949−953.

Willaert, K. W., Loewenthal, R., Sancho, J., Froeyen, M., Fersht, A., & Engelborghs, Y. (1992) *Biochemistry 31*, 711−716.

Yamamoto, Y., & Tanaka, J. (1972) *Bull. Chem. Soc. Jpn. 45*, 1362−1366.